M−F Interatomic Distances and Effective Volumes of Second and Third Transition Series MF_6^- and MF_6^{2-} Anions

Oliver Graudejus,[†] Angus P. Wilkinson,[‡] Lisa C. Chacón,[†] and Neil Bartlett*[,†]

Chemical Sciences Division, Lawrence Berkeley National Laboratory, and Chemistry Department, University of California, Berkeley, California 94720, and School of Chemistry and Biochemistry, Georgia Institute of Technology, Atlanta, Georgia, 30332

Received January 7, 2000

Synchrotron X-ray powder diffraction data (SPDD) for representative $LiMF_6$ and Li_2MF_6 salts of the second and third transition series have provided unit-cell parameters and, from Rietveld analysis, M−F interatomic distances. M−F distances have also been obtained from X-ray single-crystal structural analyses of $LiOsF_6$, Li_2PtF_6, and $KRhF_6$. The $LiMF_6$ all have the $LiSbF_6$ structure type (space group $R\bar{3}$). For M = Ta to Au the primitive unit cell volume decreases with increasing nuclear charge (Z), the volumes ($\sigma = 0.01$ Å^3) being as follows: Ta, 111.26; Os, 102.42; Ir, 100.77; Pt, 99.62; and Au, 99.12 Å^3. A similar contraction, with increase in Z, occurs from Nb to Rh, the primitive cell volume ($\sigma = 0.01$ Å^3) being: Nb, 110.92; Ru, 100.51; and Rh, 98.64 Å^3. For the TaF_6^- to AuF_6^- the M−F distances are not significantly different across the series, at ∼1.87(1) Å; also, Nb−F, Ru−F, and Rh−F = 1.86(1) Å. In each series, the a and c values of the hexagonal-cell representation for the $LiMF_6$ structure (separate layers of MF_6^- and Li^+ stacked along c) change smoothly. As Z increases, a decreases and c increases. The variation in a, like the volume change, indicates that the size of MF_6^- is decreasing with Z. The variation in c suggests that the charge on the F-ligand is decreasing with Z. In the trirutile Li_2MF_6 series, M = Mo to Pd, the formula-unit volume decreases with Z (Mo, 100.92(6); Ru, 98.21(1); Rh, 97.43(1); Pd, 96.83(1) Å^3) and a shortening in M−F occurs (Mo−F = 1.936(4); Ru−F = 1.921(7); Rh−F = 1.910(7); Pd−F = 1.899(4) Å). The less abundant data for MF_6^{2-} salts of the third transition series indicate similar trends. For both series, M−F distances of MF_6^{2-} are longer by 0.03−0.09 Å than in MF_6^-.

Introduction

The new findings from the gas-phase electron diffraction studies of the MF_6 molecules of the third transition-metal series described in the accompanying paper,[1] and especially the discovery of an abrupt increase in the M−F distance above Ir, prompted this investigation of related MF_6^- and MF_6^{2-} salts. The aim was to attempt to separate influences of the nuclear-charge (Z) and valence-electron configuration (especially from the dt_{2g}^n electron configurations) upon the M−F interatomic distance.

Fortunately, a simultaneous powder neutron diffraction study, by Marx et al.,[2] of WF_6, OsF_6, and PtF_6, found a similar increase in M−F for PtF_6, with, additionally, evidence for a small Jahn−Teller distortion in the last. X-ray absorption fine structure (XAFS) studies of the MF_6 and salts of their anions, had also been carried out earlier by Holloway and co-workers.[3] Although the latter study showed Pt−F to be longer {at 1.839(3) Å} than the other M−F distances, that of Ir−F {at 1.822(2) Å} was not found to be significantly different from W−F {1.821(2) Å}.

The Marx et al. unit cell data[2] (for 5K) also confirmed the trend, tabulated earlier by Siegel and Northrop,[4] that the unit-cell volume of the MF_6 decreases steadily with an increase in Z. This further highlighted the lengthening of the M−F distances in IrF_6, and PtF_6. The decrease in volume with the increase in Z had been commented on by one of us (N.B.), in an early attempt to correlate the oxidizing properties of MF_6 with electronic and nuclear charge effects.[5] It was noted then that the formula-unit volume of $NO^+MF_6^-$ salts, as well as MF_6, decreased with the increase in Z, in each set. At that time M−F in these MF_6 was believed to be constant. In the present studies, further investigations of volume changes and M−F distances in MF_6^- and MF_6^{2-} salts have focused on Li^+ salts. This small cation occupies octahedral-hole sites in MF_6^- and MF_6^{2-} salt structures, and salts of similar stoichiometry are often of the same structure type (this is especially so for $LiMF_6$). Additionally the small X-ray scattering factor for Li^+ improved chances of more precise structural parameters, if X-ray structural analyses were carried out.

Although we have succeeded in preparing high-purity $LiMF_6$ and Li_2MF_6 salts (the latter, especially, in the second transition series set), we have been less successful in the preparation of suitable single crystals for structural analysis. Rietveld analysis of synchrotron powder diffraction data (SPDD) has therefore been used for structural information from these salts. All have been examined on the same synchrotron line in the same diffraction arrangement. Unit-cell volume and M−F distance trends have been established for each transition series. The M−F distance findings are compared with single-crystal values from this work, for $LiOsF_6$, $KRhF_6$, and Li_2PtF_6, and with previous values from the literature.

† Lawrence Berkeley National Laboratory and University of California, Berkeley.
‡ Georgia Institute of Technology.

(1) Richardson, A.; Hedberg, K.; Lucier, G. M. *Inorg. Chem*. **2000**, *39*, 2787.
(2) Marx, R.; Seppelt, K.; Ibbertson, R. M. *J. Chem. Phys.* **1996**, *104*, 7658.
(3) Brisdon, A. K.; Holloway, J. H.; Hope, E. G.; Levason, W.; Ogden, J. S.; Saad, A. K. *J. Chem. Soc., Dalton Trans.* **1992**, 139.
(4) Siegel, S.; Northrop, D. A. *Inorg. Chem.* **1966**, *5*, 2187.
(5) Bartlett, N. *Angew. Chem., Int. Ed. Engl.* **1968**, *7*, 433.

10.1021/ic000041w CCC: $19.00
Published on Web 05/27/2000

Table 1. Crystallographic Data and Details of the Structure Determination of $LiMF_6$ (M = Nb, Ru, Rh)

(a) M = Nb, Ru, and Rh

formula	$LiNbF_6$	$LiRuF_6$	$LiRhF_6$
lattice params			
a/Å	5.31810(3)	5.07397(8)	5.02018(7)
c/Å	13.5861(2)	13.5244(3)	13.5588(3)
V/Å	332.764(4)	301.539(8)	295.931(8)
space group, *Z*	$R\bar{3}$, 3	$R\bar{3}$, 3	$R\bar{3}$, 3
temp/K	299	299	299
radiation/Å	1.282 16(2)	1.282 16(2)	1.282 16(2)
angular range (2θ)/deg	15.2−85.2	15.3−120.3	15.3−100.3
step scan increment/deg	0.01	0.015	0.01
monitor counts per step	60 000	60 000	70 000
no. of reflns	94	185	125
no. of refined params	18	18	18
peak shape	pseudo-Voigt	pseudo-Voigt	pseudo-Voigt
zero-point	−0.6093(5)	−0.6128(5)	−0.6168(3)
reliability factors			
wRp	0.131	0.117	0.101
Rp	0.099	0.074	0.069
$R(F^2)$	0.107	0.164	0.149

(b) M = Ta, Os, Ir, Pt, and Au

formula	$LiTaF_6$	$LiOsF_6$	$LiIrF_6$	$LiPtF_6$	$LiAuF_6$
lattice params					
a/Å	5.32006(8)	5.10558(6)	5.06148(4)	5.02686(4)	5.00337(5)
c/Å	13.6178(3)	13.6106(2)	13.6260(2)	13.6559(2)	13.7160(2)
V/Å^3	333.789(8)	307.256(5)	302.311(4)	298.844(4)	297.362(6)
space group, *Z*	$R\bar{3}$, 3	$R\bar{3}$, 3	$R\bar{3}$, 3	$R\bar{3}$, 3	$R\bar{3}$, 3
temp/K	299	299	299	299	299
radiation/Å	1.282 16(2)	1.282 16(2)	1.282 16(2)	1.282 16(2)	1.282 16(2)
angular range (2θ)/deg	15−127	15−114	15−115	15−117	15−106.5
step scan increment/deg	0.014	0.011	0.004	0.006	0.012
monitor counts per step	90 000	50 000	30 000	60 000	100 000
no. of reflns	217	176	173	174	150
no. of refined params	16	16	17	22	22
peak shape	pseudo-Voigt	pseudo-Voigt	pseudo-Voigt	pseudo-Voigt	pseudo-Voigt
zero-point	−0.6092(2)	−0.6086(5)	−0.5819(2)	−0.6072(5)	−0.5983(5)
reliability factors					
wRp	0.118	0.154	0.170	0.136	0.100
Rp	0.076	0.108	0.117	0.089	0.072
$R(F^2)$	0.141	0.125	0.165	0.090	0.107

Experimental Section

CAUTION: Fluorine and anhydrous HF can cause severe burns. Before undertaking work of the kind reported here, the experimentalist must become familiar with these reagents and the hazards associated with them. Fresh tubes of calcium gluconate gel should always be on hand for the fast treatment[6] of skin exposed to these reagents.

Preparation of MF_6^- and MF_6^{2-} Salts. All salts were made in liquid anhydrous HF (aHF) (Matheson Gas Products) contained in T-shaped reactors made from translucent fluorocarbon tubing (FEP) (Chemplast Inc., Wayne, NJ) and equipped with Teflon valves with Kel-F stems, provided with Teflon tips, as previously described.[7] For $LiMF_6$, M = Ta, Nb, Os, Ir, Pt, and Au, the preparations were from the elements and LiF in aHF with F_2 (photolyzed for M = Pt and Au).[8,9] For $LiMF_6$, M = Ru and Rh, equimolar quantities of the O_2RuF_6 [10] or RhF_5 [11] and LiF were placed in a previously fluorinated T reactor in the dry Ar atmosphere of a Vacuum Atmospheres Corp. DRILAB. These reagents were dissolved in aHF and mixed at ∼20 °C, the solution was decanted from any residue, and then (to help crystal growth) the aHF was slowly distilled from the solution, at ∼20 °C, to the other limb of the reactor, cooled slightly below that temperature. Li_2MF_6 salts with M = Pt, Pd, and Ru were made as described earlier,[8] and those with M = Rh, by reduction of $LiRhF_6$ following the experience of Casteel and Horwitz.[12]

Table 2. Crystallographic Data and Details of the Structure Determination of Li_2MF_6 (M = Ru, Rh, and Pd)

formula	Li_2RuF_6	Li_2RhF_6	Li_2PdF_6
lattice params			
a/Å	4.64358(6)	4.63880(8)	4.63281(4)
c/Å	9.1090(4)	9.0557(2)	9.02336(8)
V/Å^3	196.417(6)	194.865(6)	193.668(3)
space group, Z	$P4_2/mnm$, 2	$P4_2/mnm$, 2	$P4_2/mnm$, 2
temp/K	299	299	299
radiation/Å	1.28216(2)	1.28216(2)	1.28216(2)
angular range (2θ)/deg	15.1−90.1	15.2−93.2	15.2−115.2
step scan increment/deg	0.015	0.013	0.01
monitor counts per step	50 000	60 000	60 000
no. of reflns	94	160	149
no. of refined params	18	19	17
peak shape	pseudo-Voigt	pseudo-Voigt	pseudo-Voigt
zero-point	−0.6093(5)	−0.6165(5)	−0.6101(5)
reliability factors			
wRp	0.194	0.178	0.142
Rp	0.144	0.114	0.103
$R(F^2)$	0.096	0.141	0.143

Debye−Scherrer X-ray powder diffraction samples were prepared in 0.3 mm diameter quartz capillaries (Charles Supper Co., Natick, NJ) as previously described,[7] the X-ray diffraction pattern (XRDP) being

(6) For treatment of HF injuries, see: Finkel, A. In *Advances in Fluorine Chemistry;* Tatlow, J. C., Peacock, R. D., Hyman, H. H., Eds.; Butterworth and Co. Ltd.; London, 1973; Vol. 7, pp 199−203.

(7) Zemva, B.; Hagiwara, R.; Casteel, W. J., Jr.; Lutar, K.; Jesih, A.; Bartlett, N. *J. Am. Chem. Soc.* **1990**, *112*, 4846.

(8) Lucier, G. M.; Elder, S. H.; Chacón, L. C.; Bartlett, N. *Eur. J. Solid State Inorg. Chem.* **1996**, *33*, 4846.

(9) Graudejus, O.; Elder, S. H.; Lucier, G. M.; Shen, C.; Bartlett, N. *Inorg. Chem.* **1999**, *38*, 2503.

(10) Edwards, E. J.; Falconer, W. E.; Griffiths, J. E.; Sunder, W. A.; Vasile, M. J. *J. Chem. Soc., Dalton Trans.* **1974**, 1129.

(11) Holloway, J. H.; Rao, P. R.; Bartlett, N. *Chem. Commun.* **1965**, 393.

(12) Casteel, W. J., Jr.; Horwitz, T. *Eur. J. Solid State Inorg. Chem.* **1992**, *29*, 649.

Table 3. Crystallographic Data for $LiOsF_6$ (Room- and Low-Temperature Data), $KRhF_6$, and Li_2PtF_6

formula	$LiOsF_6$	$LiOsF_6$	$KRhF_6$	Li_2PtF_6
formula wt	311.13	311.13	255.994	322.96
lattice params				
a/Å	5.1111(8)	5.0512(3)	7.4060(2)	4.6378(2)
c/Å	13.625(4)	13.5932(9)	7.2714(2)	9.100(4)
V/Å^3	308.2(2)	300.36(6)	345.39(1)	195.74(5)
space group, Z	$R\bar{3}$, 3	$R\bar{3}$, 3	$R\bar{3}$, 3	$P4_2/mnm$, 2
d_{calc}/(g·cm^{-3})	5.028	5.160	3.692	5.479
F(000)	399	399	354	276
μ(Mo Kα)/cm^{-1}	310.6	318.7	46.39	357.35
radiation	Mo Kα	Mo Kα	Mo Kα	Mo Kα
temp/K	293	129	158	129
no. of measd unique reflns	130	280	520	404
R_{int}	0.0758	0.0426	0.025	0.035
residuals: R1,[a] wR2[b]	0.0315, 0.0789	0.0249, 0.0602	0.026, 0.032	0.049, 0.062
goodness of fit	1.232	1.071	1.36	2.75
max/min peak in final diff map/(Å^3·e^{-1})	+1.78/−2.76	+2.57/−7.59	+1.45/−1.36	+8.39/−5.27

[a] $R1 = \sum||F_o| - |F_c||/\sum|F_o|$. [b] $wR2 = [\sum w(|F_o|) - |F_c|)^2/\sum wF_o^2]^{1/2}$.

recorded on film using Ni-filtered Cu Kα radiation (General Electric Co. precision camera, Straumanis loading). The program ERACEL[13] was used for the refinement of the lattice parameters which incorporates the Nelson−Riley extrapolation function.[14] Each $LiMF_6$ compound was indexed on the basis of a trigonal-rhombohedral unit cell ($LiSbF_6$-type, $R\bar{3}$, for the hexaonal unit-cell representation, $Z = 3$; see Table 1). Those microcrystalline Li_2MF_6 salts investigated here (M = Ru, Rh, Pd) crystallize in the trirutile structure[15] ($P4_2/mnm$, $Z = 2$, see Table 2).

For the synchrotron radiation powder diffraction experiments, 0.3 mm o.d. quartz capillaries were filled to a length of about 1 cm with the sample. The powder was finally tamped down into a well-packed column with a glass ram-rod drawn down to fit the 0.3 mm capillaries. Loaded capillaries were plugged with Kel-F grease, removed from the DRILAB, and sealed by drawing down in a small flame.

Synchrotron-radiation powder diffraction data (SPDD) were collected on the 2−1 beamline at the Stanford Synchrotron Radiation Laborotry (SSRL) of Stanford University. With a silicon standard, the wavelength was determined to be 1.281 26 Å.

Structure Refinements with SPDD. The refinement of the structures of the $LiMF_6$ and Li_2MF_6 was accomplished using the program GSAS.[16] The starting atom positions for the refinement of the powder data were obtained from the single-crystal data of $LiOsF_6$ and Li_2PtF_6, given below. Initial lattice parameters were derived from Debye−Scherrer XRDPs of the respective compounds. After a background correction had been applied, the lattice parameters and the zero point of the patterns were refined. Afterwards the profile and atom positions were obtained. A Debye−Scherrer absorption correction was applied to both data sets, assuming a packing density of the powder of about 40−50%. The correction was applied within the program GSAS[13] using an empirical function developed by N. N. Lobanov (personal communication to A.P.W.). This function reproduces the required absorption correction within 1% for cylindrical samples with $\mu R < 30$. A small impurity in the pattern of $LiNbF_6$, $LiRuF_6$, and Li_2RuF_6 was probably due to some hydrofluoride of lithium. Crystallographic data and details of the structure determinations are given, for $LiMF_6$ (M = Nb, Ru, and Rh) in Table 1a, for $LiMF_6$ (M = Ta, Os, Ir, Pt, and Au) in Table 1b, and for Li_2MF_6 (M = Ru, Rh, Pd) in Table 2. Positional and thermal parameters for the $LiMF_6$ salts are given in Table S1 (Supporting Information), and those for the Li_2MF_6 salts in Table S2. The observed SPDD patterns, together with the calculated values from the best fit, a difference curve ($I_{obs} - I_{calc}$), and the reflection positions are shown for each salt in Figures S3−S13 (Supporting Information).

Single-Crystal Structures for $LiOsF_6$, $KRhF_6$, and Li_2PtF_6. Single crystals suitable for structural analysis were grown by the method described above under Preparations. Crystals of the respective compounds were mounted in 0.3 mm o.d quarz capillaries. $KRhF_6$ and $LiOsF_6$ are very sensitive to moisture and have to be manipulated in the dry Ar atmosphere of a drybox. Li_2PtF_6 is insensitive to water at ambient temperature and can be handled in the atmosphere without decomposition. The crystals used in the structure determinations are described, and other pertinent data given, in Table S14 (Supporting Information).

All measurements were carried out on a SMART diffractometer with graphite monochromated Mo Kα radiation.

Single-Crystal Structural Solutions and Refinements. Each structure was solved with the aid of the isotype structure ($LiSbF_6$ type,[17] $KOsF_6$ type,[18] trirutile type[15]).

$KRhF_6$. It was impossible to get an accurate measurement of the crystal size because the crystal was dislodged following data collection and could not be found. Frames corresponding to 97% complete coverage to a resolution of 0.54 Å at an average redundancy of 2.1 were collected using scans of 0.30° counted for a total of 30 s each. Data were integrated using the program SAINT[19] with box parameters of 1.6 × 1.6 × 0.6° to a maximum 2θ value of 83.7°. No decay correction was applied. A correction for secondary extinction was applied (coefficient = 2.2(3) × 10^{-6}). The structure was solved by direct methods and expanded using Fourier techniques.

Li_2PtF_6. The structure refinement was very sensitive to the exact value of the absorption correction, especially the value of μR, which determines the variation of the absorption correction in sin θ/λ. The value of μR was correlated to the value of the extinction parameter and to the final R-value. The selection of the final value was based in part on the R-value and in part on a "reasonable" value for the extinction. This effect was exacerbated by the low number of observed reflections with $h + k + l \neq 2n$. The Pt−F distances are of low accuracy (±0.01 Å) because most of the reflections with $h + k + l \neq 2n$ are "unobserved" even at the 2σ level. Of the approximately 200 reflections in that class, only 21 are greater than 2σ, and presumably most of these are at low sin θ/λ. Since the intensities of the body-centered reflections are primarily determined by the Pt atoms, the fluorine positions are critically affected by the anti-body-centered reflections, which are poorly determined. The final empirical absorption correction based on comparison of redundant and equivalent refelctions was applied with the program SADABS.[20] The critical value of μR was adjusted manually to give the lowest residuals in least squares.

$LiOsF_6$. The structure was refined using the atom positions of $LiSbF_6$ (with which $LiOsF_6$ is isostructural)[17] as starting parameters. The refinement proceeded without any difficulty and converged after a few cycles.

(13) Laugier, J.; Filhol, A. Local version of program CELREF, Nantes; 1978.
(14) Nelson, J. B.; Riley, D. P. *Proc. Phys. Soc.; London* **1945**, *57*, 160.
(15) Portier, J.; Menil, F.; Hagenmuller, P. *Bull. Soc. Chim.* **1970**, *10*, 3485.
(16) Larson, A. C.; Von Dreele, R. B. *Los Alamos National Laboratory Report No. LA-UR-86-748*; Los Alamos National Laboratory: 1987.
(17) Burns, J. H. *Acta Crystallogr.* **1962**, *15*, 1098.
(18) Hepworth, M. A.; Jack, K. H.; Westland, G. J. *J. Inorg. Nucl. Chem.* **1956**, *2*, 79.
(19) *SAX Area-Detector Integration Program*, V4.024; Siemens Industrial Automation, Inc.: Madison, WI, 1995.
(20) Siemens Area Detector ABSorption correction program: Sheldrick, G. Advance copy, private communication, 1996.

Table 4. M−F Interatomic Distances (Å) in Third Transition Series MF_6, MF_6^-, and MF_6^{2-} and M−F Stretching Force Constants for MF_6 Molecules[a] (f_{M-F}, $cm^{-1}/cÅ^2$)

M	Hf	Ta	W	Re	Os	Ir	Pt	Au
MF_6[b]			1.829(2)	1.829(2)	1.828(2)	1.839(2)	1.851(2)	
f_{M-F}			26.480	26.353	26.185	25.181	23.033	
$[MF_6]^-$ [c]		1.859(4)			1.872(7)	1.879(5)	1.887(6)	1.874(6)
$[MF_6]^-$ other		1.86(1)[d]		1.863(4)[e]	1.879(4)[f]	1.875(3)[g]	1.873(6)[h]	1.890(4)[i]
$[MF_6]^{2-}$	1.991[j]			1.953(4)[k]		1.939(6)[l]	1.92(1)[m]	

[a] Weinstock, B.; Goodman, G. L. In *Advances in Chemical Physics*; Prigogine, I., Ed.; Interscience Publishers: London, New York, 1965; Vol. IX, pp 169−319. [b] Reference 1. [c] Synchrotron radiation X-ray diffraction data. [d] In NH_4TaF_6: Grimberg, C.; Strähle, J.; Laval, J. P.; Frit, B.; Sonntag, R.; Ihringer, J. *Eur. J. Solid State Inorg. Chem.* **1994**, *31*, 449 (powder neutron data). [e] In $CsReF_6$: Hoskins, B. F.; Linden, A.; Mulvaney, P. C.; O'Donnell, T. A. *Inorg. Chim. Acta* **1984**, *88*, 217 (single-crystal data). [f] In $LiOsF_6$ (single-crystal data at 129 K). [g] In $LiIrF_6$: Graudejus, O.; Fitz, H., to be published (single-crystal data). [h] In $CsPtF_6$: Fischer, R.; Müller, B. G., to be published (single-crystal data). [i] In O_2AuF_6: Graudejus, O.; Müller, B. G. *Z. Anorg. Allg. Chem.* **1996**, *622*, 1076 (single-crystal data). [j] In $CaHfF_6$: ref 26 (single-crystal data). [k] In K_2ReF_6: ref 27 (single-crystal data). [l] In K_2IrF_6: ref *g* (single-crystal data). [m] In Li_2PtF_6 (single-crystal data at 129 K). Diffraction data were collected at ∼293 K unless specified otherwise.

Neutral atom scattering factors were taken from Cromer and Weber.[21] Anomalous dispersion effects[22] were included in F_c, and the values for f' and f'' were those of Creagh and McAuley.[23] The values for the mass attenuation coefficients are those of Creagh and Hubbell.[24] All calculations were performed using the teXsan[25] crystallographic software package of Molecular Structure Corp. All data were corrected for Lorentz and polarization effects. An empirical absorption correction based on comparison of redundant and equivalent data and an ellipsoidal model of the absorption surface was applied to all data using the program SADABS.[20] Final unit-cell parameters are in Table 3, and atomic coordinates and thermal parameters, in Tables S15 and S16 (Supporting Information). Interatomic distances and angles are in Tables S17 and S18.

Results and Discussion

Synchrotron X-ray data for the $LiMF_6$ salts given in Table 1 show the formula-unit volume decreasing steadily with the increase in *Z*. In addition, from the *c* and *a* values of the hexagonal-cell representation, the *c* values are seen to increase slightly with *Z* as the *a* values decrease. This structure is illustrated in Figure 1. It is in essence a layer structure of MF_6^- and Li^+. The decrease in *a* across the series indicates a decrease in the effective packing diameter of MF_6^-. Because the diameter of MF_6^- must also be a component of *c*, the latter would be expected to contract with the increase in *Z*, if the charge on the F-ligands were constant. The small increase in *c*, with the increase in *Z*, suggests decreasing attraction between the Li^+ and the MF_6^- (alternating layers, along *c*) perhaps because of increasing polarization of the F^- ligand charge by M as *Z* increases. Unfortunately there was no general success in growing single crystals of these salts; therefore, we depend on structural findings from a variety of salts, for the M−F distances in these anions given in Table 4. To check at least the relative changes in M−F across the series, however, powder synchrotron data were collected and subjected to Rietveld analysis. These findings are also included in Table 4. The formula-unit volumes (FUVs) and M−F distances are illustrated for the second and third transition series in Figures 2 and 3.

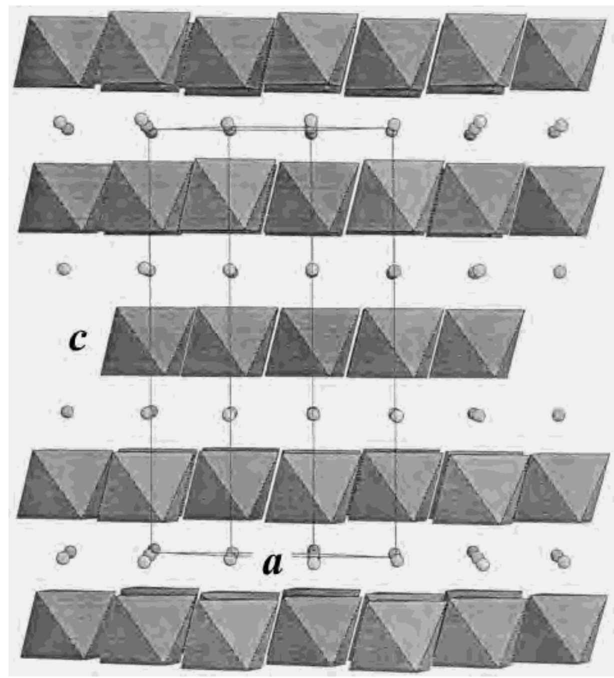

Figure 1. View of the $LiSbF_6$ structure perpendicular to the *c*-axis.

Although one could have wished for more precision in some cases, there is no significant change in the M−F distances of MF_6^-, from M = Ta to Au, none being significantly different from 1.87(1) Å. This is also in harmony with the XAFS findings (on KMF_6 salts) for Os−F and Pt−F {1.882(2) and 1.886(2) Å} of Holloway and co-workers[3] but not for their Ir−F value {1.910(2) Å}. In these electron-rich relatives of the MF_6 molecules, therefore, there is no analogous increase in M−F distance at the t_{2g}^3 configuration and beyond. It is also clear that the addition of an electron to MF_6 to make an anion, MF_6^-, always increases M−F, although less so for Pt−F and Ir−F than the other members of the series. The approximate constancy of M−F distances in the MF_6^- contrasts with the steady decrease in FUV and effective packing diameter, in the $LiMF_6$ salts (see Table 1b). It is, therefore, apparent that the van der Waals radii of the MF_6^- are diminishing with *Z*. This suggests that the nonbonding F-ligand electron density projecting trans to the M−F bond is being contracted by increasing *Z*.

(21) Cromer, D. T.; Weber, J. T. *International Tables for X-ray Crystallography;* The Kynoch Press; Birmingham, England, 1974; Vol. IV, Table 2.2A.
(22) Ibers, J. A.; Hamilton, W. C. *Acta Crystallogr.* **1964**, *17*, 781.
(23) Creagh, D. C.; McAuley, W. J. In *International Tables for X-ray Crystallography;* Wilson, A. J. C., Ed.; Kluwer Academic Publishers; Boston, MA, 1992; Vol. C, Table 4.2.6.8, pp 219−222.
(24) Creagh, D. C.; Hubbell, J. H. In *International Tables for X-ray Crystallography;* Wilson, A. J. C., Ed.; Kluwer Academic Publishers; Boston, MA, 1992; Vol. C, Table 4.2.4.3, pp 200−206.
(25) *teXsan: Crystal Structure Analysis Package*; Molecular Structure Corp.: The Woodlands, TX, 1985 and 1992.
(26) Graudejus, O. Unpublished result.
(27) Clark, G. R.; Russell, D. R. *Acta Crystallogr.* **1978**, *B34*, 894.
(28) Casteel, W. J., Jr.; Wilkinson, A. P.; Borrmann, H.; Serfass, R. E.; Bartlett, N. *Inorg. Chem.* **1992**, *31*, 3124.
(29) Gundersen, G.; Heldberg, K.; Strand, G. *J. Chem. Phys*. **1978**, *68*, 3548.
(30) Gafner, G.; Kruger, C. J. *Acta Crystallogr*. **1974**, *30*, 250.
(31) Bartell, L. S.; Anding, J. *J. Mol. Struct*. **1984**, *118*, 47.
(32) Borrmann, H.; Whalen, J. M. Private communication to N.B.

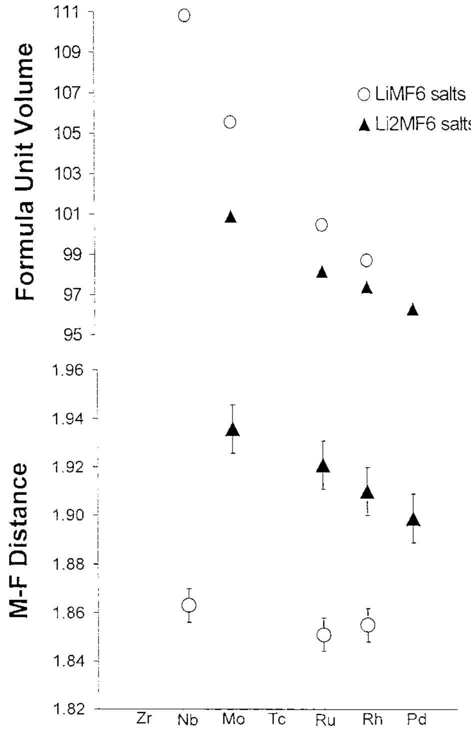

Figure 2. Comparison of M−F interatomic distances (±σ) and formula unit volumes for second transition series MF_6^- and MF_6^{2-}.

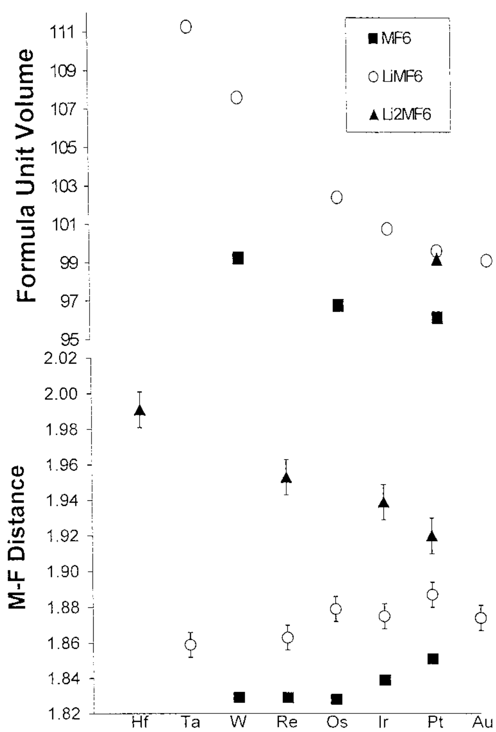

Figure 3. Comparison of M−F interatomic distances (±σ) and formula unit volumes for third transition series MF_6, MF_6^-, and MF_6^{2-}.

Addition of an electron to MF_6^-, to give MF_6^{2-} (see Table 4), also increases M−F, with M^{IV}−F distances decreasing from Hf−F = 1.991 Å,[26] through Re−F = 1.953(4) Å[27] to Pt−F = 1.92(1) Å. Therefore, both in the formation of MF_6^- and MF_6^{2-}, the addition of an electron leads to an increase in the interatomic M−F distance. Evidently in the MF_6^- series the nuclear charge increase neatly balances the impact of an added electron. With the MF_6^{2-} series, however, it appears that the contracting effect of the nuclear charge increase slightly exceeds the impact of the M−F lengthening influence of added dt_{2g} electrons. These dianions are, however, more electron rich and longer bonded, and are therefore more easily contracted than MF_6^-. (A study of M−F distances[28] in the second and third transition series binary fluorides has indicated the importance of hard-sphere F−F repulsions in setting those distances.) Roughly stated, however, the impact of an added electron, for a given M, in either set (MF_6 or MF_6^-) of the third transition series, is to increase the M−F distance by ~0.03 Å (high Z, n = 0 to 1) to ~0.09 Å (low Z, n = 1 to 2). Such an increase is offset in crossing either the MF_6 or MF_6^- series, by an approximately equal contraction due to the increase in Z. It is of significance that a contraction of M−F with nuclear-charge increase occurs in isoelectronic non-transition-element species.

For $LiSbF_6$, with[17] Sb−F = 1.88 ± 0.02 Å, we have an interatomic distance very like those of the second and third transition series MF_6^-. In particular, the unit-cell dimensions of $LiSbF_6$ (a = 5.18 ± 0.02 Å, c = 13.60 ± 0.02 Å)[17] and $LiOsF_6$ (see Table 1) are similar and the Os−F distance from the single-crystal structure is 1.879(4) Å. The isoelectronic relative of SbF_6^-, of one unit of Z higher nuclear charge, TeF_6, has[29] Te−F = 1.815(2) Å, i.e. a contraction of ~0.06 Å from Sb−F. For the smaller AsF_6^- and SeF_6 isoelectronic pair, the impact of increasing Z is smaller with[30] As−F = 1.719(3) and[31] Se−F = 1.685(2) Å. The contraction in passing from TeF_6 to IF_6^+ (I−F = 1.780(5) Å)[32] is also smaller (~0.035 Å). These smaller contractions with increase in Z in the smaller species probably reflect greater F-ligand−F-ligand repulsion. It should also be noted that the vibrational spectroscopic data[33] for nearly isodimensional species such as TeF_6 and WF_6 (M−F stretching force constants: Te−F, 26.032; W−F, 26.480 $cm^{-1}/cÅ^2$) indicate that the intrinsic bond strengths must also be similar. This similarity indicates that *the nature of the bonding in TeF_6 and WF_6 is essentially the same*. The simple ionic bonding model accounts straightforwardly for the physical and chemical properties of these and related hexafluorides. Although not even the highest level *ab initio* calculations for the MF_6 molecules precisely reproduced the experimental M−F distance values, or the exact dependence of those values on Z (see accompanying paper[1]), those calculations do indicate that the bonding is highly ionic. The Mulliken charge for the metal-atom center (except for the Pt case, which is slightly lower) exceeds +4, the F-ligand charge being nearly −0.7.

As was first pointed out by Moffitt et al.[34] ligand-field theory (with a central M^{6+} surrounded octahedrally by six F^-) provides a detailed classification of the electronic states of lowest energy in the third transition series MF_6 molecules. In their excellent accounting for the details of the electronic spectra of these hexafluorides they pointed out that the coupling scheme obeyed by the "nonbonding" valence electrons is dominated by the electric field, the Coulomb correlation and the spin−orbit energies contributing about equally, with about one-tenth of the value of $10Dq$. They concluded that the ligand field is very strong in this set, with $10Dq$ 30 000 cm^{-1}, the ground and low-lying excited electronic states arising from the same configuration $(dt_{2g})^n$. Their theoretical evaluation did not, however, inform us of the remarkable electron affinities[5,35] of these molecules.

(33) Weinstock, B.; Goodman, G. L. In *Advances in Chemical Physics*; Prigogine, I., Ed.; Interscience Publishers: London, New York, 1965; Vol. IX, pp 169−319.
(34) Moffitt, W.; Goodman, G. L.; Fred, M.; Weinstock, B. *Mol. Phys.* **1959**, *2*, 109.
(35) George, P. M.; Beauchamp, J. L. *Chem. Phys.* **1979**, *36*, 345.

Each of IrF_6 and PtF_6 is able to liberate elemental fluorine in interaction with gaseous ONF at room temperatures,[5,36] and PtF_6 can take an electron from O_2 [37] or Xe.[38] Indeed, these are merely the most spectacular oxidations, of the highest Z MF_6. Comparitive study of the whole set of MF_6 showed[5] that the electron affinity of MF_6 $\{E(MF_6)\}$ increased by ~1 eV, for each unit increase in Z. The straightforward explanation for this linear dependence of $E(MF_6)$ on Z is to place the added electron in an orbital dt_{2g} that is largely centered on M, since each electron centered on M then experiences one unit of nuclear charge more than does its counterpart in the immediately preceding MF_6. We must also accept that each of the dt_{2g} electrons of the neutral MF_6 of the third transition series shields the nuclear charge in such a way that the intrinsic M−F bond strength, as reflected in the M−F distance and the stretching force constants,[33] remains very nearly the same across the series from M = W to Os. Simultaneously, we must also explain the observed formula volume contraction for each set of MF_6, MF_6^-, and MF_6^{2-}.

The FUV contraction with the increase in Z can be accounted for in a displacement of the σ M−F bonding electron pair toward M as the Z of M increases. Contraction of the M−F distance does not occur because of the π^* influence of the $(dt_{2g})^n$ configuration. It follows that the F-ligand is less negatively charged at higher Z of M, and its electron clouds more contracted, including those trans to the M−F bonds. The latter, especially, affect the van der Waals radius. In the case of electron addition to a given MF_6^{n-} (n = 0, or 1) the π^* effect of $(dt_{2g})^n$ alone is dominant. To that must be attributed the increase in the M−F distance per added electron of ~0.03 Å (high Z, n = 0 to 1) to ~0.09 Å (low Z, n = 1 to 2). Indeed, the only remaining set of observations to still account for is the increase in M−F (at higher Z than that in OsF_6) in the MF_6 molecules.

As has already been remarked, IrF_6 and PtF_6 are able to liberate elemental F_2 in interaction with fluorides. It is therefore plausible to assume that the energy levels of the $(dt_{2g})^n$ orbitals are close to those of the nonbonding F-ligand orbitals in these molecules, and especially in PtF_6, nearly degenerate with them, such that electron transfer from the latter orbitals to the dt_{2g} orbitals easily occurs. Although the MF_6 molecule computations[1] did not conform precisely with the experimental findings, it may be significant that the Mulliken charges for M in the best *ab initio* calculations had the following positive values: W, 4.08; Re, 4.08; Os, 4.32; Ir, 4.24; Pt, 3.85. The decrease in the values from Os to Pt is consonant with the postulated charge transfer in IrF_6 and PtF_6. As we shall argue, the onset of the F-ligand to M charge-transfer must occur earlier in the second transition series.

It is clear from the volume and M−F distance data, for $LiMF_6$ and Li_2MF_6 salts, given in Tables 1, 2, 4, and 5 that the effective nuclear charge increases more sharply across the second transition series than across the third. This is in line with the higher ionization potentials[39] for the ionization of the 4d electrons, compared to their 5d relatives, and is connected to a well-known relativistic effect.[40,41] Remarkable oxidizing properties appear earlier in the second series. Thus, MoF_6 oxidizes NO to give a $NO^+MF_6^-$ salt,[42] whereas WF_6 does not oxidize it. Also, already in RuF_6 we have a molecule capable of oxidizing O_2, to give[43] $O_2^+RuF_6^-$. Unfortunately, although RuF_6 and RhF_6 can now be made relatively easily[44,45] from aHF solution, neither is easily separated from the HF, so the electron diffraction studies of them have not yet been carried out. It is clear, however, that, for such powerful oxidizers, electron capture by M^{6+}, as in PtF_6, must result in a lengthening of the Ru−F and Rh−F distances over that observed for Mo−F, in MoF_6. It is seen from the stretching force constants of Weinstock and Goodman,[33] given in Tables 4 and 5, that the force constants of the Mo−Rh set of MF_6 show a steady decrease with Z, whereas a sizable decrease does not occur for the third transition series set until the longer bonded IrF_6 and PtF_6 are reached. The EXAFS findings of Holloway and co-workers[46] for the second transition series hexafluoro species indicate that an increase in M−F with Z does indeed occur. Their M−F distances are as follows: Mo−F = 1.809(1); Ru−F = 1.824(2); Rh−F = 1.838 Å. For the MF_6^- and MF_6^{2-} salts, their M−F distances (M = Mo, Ru, Rh) show no such increase with Z and differ only slightly from our values (given in Table 5). It may also be pertinent that RuF_6 and RhF_6, like PtF_6, are deep-red gases. This strong color is probably associated with our conjectured charge transfer from the F-ligands to the metal-ion core. The M^{6+} in RhF_6 probably possesses the highest effective nuclear charge of any hexafluoride, and even in the RhF_6^- species there may be electron transfer, from the ligands to the Rh^{5+}. That would explain the dark red color of all of the salts of that ion. Very high effective nuclear charge at the Pd-atom center, and poor screening of that charge by the $(dt_{2g})^n$ electrons, must be the reasons for the failure of all attempts to prepare PdF_6, or even PdF_6^-. For similar reasons AuF_6 has also foiled all attempts at its synthesis, but the less dramatic impact of increasing Z on the electronegativity of the M^{6+} in the third transition series gives some hope that this molecule (which will surely lose fluorine with small thermal excitation) may eventually be prepared. Because of high effective Z, the π^* influence of the dt_{2g}^6 configuration, and the consequent high electrone-

Table 5. M−F Interatomic Distances (Å) in Second Transition Series $LiMF_6$ and Li_2MF_6 Salts and M−F Stretching Force Constants for MF_6 Molecules[a] (f_{M-F}, $cm^{-1}/cÅ^2$)

M	Nb	Mo	Ru	Rh	Pd
MF_6 f_{M-F}		24.673	23.304	21.770	
$MF_6^{-\ b}$	1.863(3)		1.851(8)	1.855(5)	
$MF_6^{-\ c}$			1.851(2)[d]	1.853(1)[e]	
$MF_6^{2-\ b,f}$			1.921(7)	1.910(7)	1.899(4)
$MF_6^{2-\ c,f}$		1.936(4)[g]		1.907(4)[h]	

[a] Reference 33. [b] M−F distances from synchrotron radiation X-ray diffraction data. [c] Single-crystal data. [d] In O_2RuF_6 (at 146 K): Botkovitz, P.; Lucier, G. M.; Rao, R. P.; Bartlett, N. *Acta Chim. Slov.* **1999**, *46*, 141. [e] In $LiRhF_6$: Graudejus, O.; Fitz, H., to be published; in $KRhF_6$ at 158 K, 1.853(2) Å. [f] Values are averaged since they are not required to be the same by symmetry. [g] In Li_2MoF_6: Baur, W. H. *Acta Crystallogr.* **1994**, *B50*, 141. [h] In Li_2RhF_6: ref *e*.

(36) Bartlett, N.; Beaton, S. P.; Jha, N. K. *Chem. Commun.* **1966**, 168.
(37) Bartlett, N.; Lohmann, D. H. *Proc. Chem. Soc.* **1962**, 277; *J. Chem. Soc.* **1962**, 5253.
(38) Bartlett, N. *Proc. Chem. Soc.* **1962**, 218.
(39) Moore, C. E. *Ionization Potentials and Ionization Limits Derived from the Analysis of Optical Spectra*; NRDS-NBS 34; National Bureau of Standards: Washington, D.C., 1970.
(40) Pitzer, K. S. *Acc. Chem. Res.* **1979**, *12*, 271.
(41) Pyykkö, P.; Desclaux, J.-P. *Acc. Chem. Res.* **1979**, *12*, 276.
(42) Gleichmann, J. R.; Smith, E. A.; Trond, S. S.; Ogle, P. R. *Inorg. Chem.* **1962**, *1*, 661.
(43) Edwards, A. J.; Falconer, W. E.; Griffiths, J. E.; Sunder, W. A.; Vasile, M. J. *J. Chem. Soc., Dalton Trans.* **1974**, 1129.
(44) Lucier, G. M.; Shen, C.; Casteel, W. J., Jr.; Chacón, L.; Bartlett, N. *J. Fluorine Chem.* **1995**, *72*, 157.
(45) Lucier, G. M. Ph. D. Thesis, University of California, Berkeley, 1995; *Lawrence Berkeley Laboratory Report*, "Synthesis, Structure, and Reactivity of High Oxidation State Silver Fluorides and Related Compounds", LBL-37334, UC-401; Lawrence Berkeley Laboratory: Berkeley, CA.
(46) Brisdon, A. K.; Holloway, J. H.; Hope, E. G.; Levason, W.; Ogden, J. S.; Saad, A. K. *J. Chem. Soc., Dalton, Trans.* **1992**, 447.

gativity of the Hg^{VI}, it appears unlikely that HgF_6 can be prepared.

Acknowledgment. The authors gratefully acknowledge support from the National Science Foundation, Grant No. DMR-9404755, and the Director, Office of Energy Research, Office of Basic Energy Sciences, Chemical Science and Materials Science Divisions of the U. S. Department of Energy under Contract No. DE-AC-03-76SF00098. O.G. gratefully acknowledges the Alexander Humboldt Foundation for a Feodor-Lynen Fellowship. L.C.C. is grateful to NPSC for a fellowship. Work involving the collection of powder diffraction was carried out under the auspices of the Stanford Synchrotron Radiation Laboratory, which is operated by the Department of Energy, Office of Basic Energy Sciences.

Supporting Information Available: Tables listing of positional and thermal parameters of single crystal and powder diffraction data, X-ray experimental details, and interatomic distances and figures showing Rietveld plots. This material is available free of charge via the Internet at http://pubs.acs.org.

IC000041W